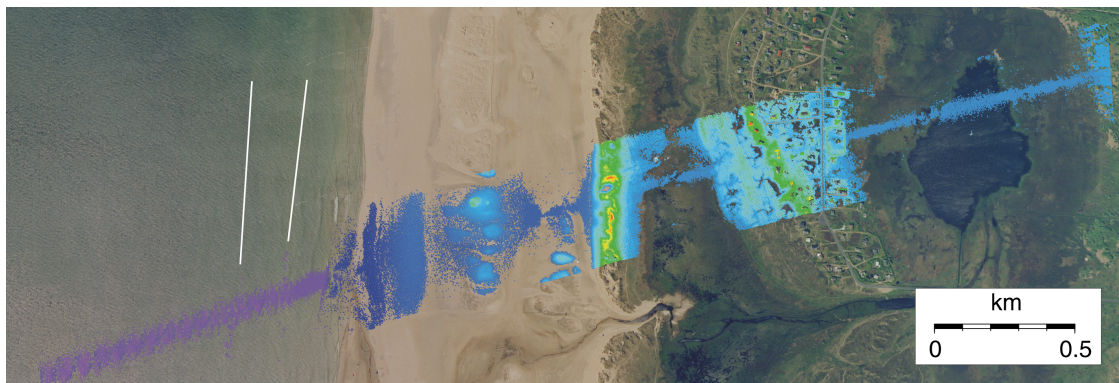# Airborne Laser Scanning Survey of the Wadden Sea Region, Denmark

Christian J. Andersen, Nynne S. Dalå, René Forsberg,
Sine M. Hvidegaard and Kristian Keller

Abstract

This report describes the results and findings of a single day airborne laser scanning survey from the Danish Wadden Sea region on March 5, 2002. The hardware used is a fairly new and relatively low-priced system comprising a Riegl laser sensor, a GPS and an INS system, mounted in a fixed-winged aircraft. The system is owned and operated by the Danish National Space Center (DNSC).

Approximately 20.6 million georeferenced elevations were obtained from three locations: An area northeast of Viborg, an area including Roskilde airport and from the main focus of the survey, the Danish Wadden Sea. The data was gathered to gain experience on accuracy and usefulness of the Riegl laser scanner for beach mapping and general usefulness for height mapping in Denmark.

One goal was to asses the applicability of airborne laser scanning (ALS) in the littoral region. Although reflectance of the laser signal on the sub-aerial beach is hindered by water, some coastal features could be observed. Two coastal bars and a beach furrow were identified.

The processing of the laser data was primarily done with software developed *in-house* (READEGI, GPSEGI and READSCAN) except the kinematic GPS solution, which was achieved using Trimble's GPSurvey.

The quality of the DEM is good and most structures are represented in good detail. Three different methods to obtain ground truth were developed and evaluated. We conclude that the LiDAR derived elevations have a high degree of precision. Precision is on the 10 cm level, as should be expected for kinematic GPS, which is believed to be the main contributor to the error budget.

Keywords: Airborne Laser Scanning, LiDAR, Wadden Sea, DEM

Contents

List of Figures

Chapter 1

Introduction

1.1   The Wadden Sea Region

The Wadden Sea is the name given to the Northwest European coastal plain estuary environment, extending from Den Helder in the Netherlands to Blåvands Huk in Denmark. It is a system of sandy barrier islands situated on a low gradient glacial outwash plain. The shallow water coastal lagunes behind the barriers are influenced by tide. Typically $^2/_3$ of these back-barrier tidal bassins are laid dry at neap tide. The tidal regime in the Danish Wadden Sea is characterised by an amphidromous system lying to the west in the North Sea. The system describes how the Atlantic tidal wave divides, one part going through the English channel, the other around the British Isles, heading south down the Scottish and English North Sea coast. The two tidal waves meet in the North Sea, resembling of stationary wave rotating anti-clockwise. The tides in the Danish Wadden Sea are semidiurnal and micro-tidal, having a mean tidal range of 1.5 m (Christiansen et al., 2004), though meterological forced sea level variation is higher. The barrier islands are exposed to the moderately high energy wind wave climate of the North Sea with mean annual off-shore wave heighs of 0.6 m and storm waves that can exceed 5 m (Christiansen et al., 2004). Because of the gentle slope of the beach profile, waves dissipate most of their energy, breaking over 2-3 coastal bars, before reaching the coastline.

Sandy barriers are a common feature around the world's shorelines and are often extensively exploited for recreational activities. Barriers are also one of the most dynamic coastal elements, being vulnerable to depletion of off-shore sources, sea level rise and human interference (Bird, 1993). The area is subject to monitoring and assesment by the trilateral expert group, the Coastal Protection and Sea Level Rise Group (CPSL), attended by The Netherlands, Germany and Denmark. The purpose is to monitor and asses the impact of climatic change, sea level rise and human activity, on the morphology and the biodiversity of the system. Nielsen and Nielsen (2002) has reported a sea-level rise of 4.21 mm/year over the last 25 years.

1.2   LiDAR

LiDAR (Light Detection and Ranging) sensors were originally developed by the US navy to assist in submarine detection, and started as simple laser profilers, pointing downwards in the nadir direction. Later the scanning laser was developed producing a swath over the terrain overflown. Lasers can divert the laser pulses across the track in different ways. The most common method is

to deflect the pulses by a rotating mirror. Another type of LiDAR sensor is the Falcon sensor developed by the german company TopoSys. This fiber scanner concept is based on a fixed linear array of fibers which sends the laser beams in fixed directions to the ground.

LiDAR sensors uses two different ranging principles. Most common are the pulsed laser systems, measuring the travelling time from the laser aperture to the target surface and back to the photo receiver (two way ranging). In some terrain types e.g. vegetation, a laser pulse will have several returns. In response to this some systems record all the discrete returns, resulting in a comprehensive sampling of the return signal, referred to as full wave sampling.

Some systems use continuous wave detection. In continuous wave (cw) laser ranging the laser intensity is modulated with a well defined function, e.g. a sinusoidal or a square wave signal. The laser emits continuously with moderate average power levels. The time of flight of the signal is determined by measuring the phase difference between the transmitted and received signal.

Lasers produce electro magnetic radiation of a specific wavelengh (λ), depending on the specific type of laser. It is useful to distinguish between red (and near infra-red) lasers and green lasers. This is due to the fact that red lasers are reflected by water whereas green lasers are not. A few companies utilize green lasers in airborne laser bathymetry (ALB).

Because of the high precision of LiDAR systems they have found use in many different fields. Terrestrial systems are used in forestry and construction. Airborne laser scanning (ALS) has the advantage of being cost-efficient compared to traditional on-the-ground surveying. Using ALS, thickness of sea-ice and heights of inland ice are monitored in Greenland (Forsberg et al., 2001; Keller et al., 2004). In Switzerland LiDAR has been used to monitor mass balance of glaciers (Geist and Stötter, 2004). Fault lines and scarps have been identified from LiDAR imagery in Seattle, USA (Haugerud et al., 2003). In the field of archeology, fossilized ridge and furrow structures from the 15th century, have been identified through dense forest canopy (Sittler, 2004). The Dutch ministry of public works (Rijkwaterstaat) is using LiDAR to monitor erosion on the sub-aerial beach, along the Dutch North Sea coast. Holland is also the first country to be completely covered by a LiDAR digital elevation model (DEM)(Maas, 2002). LiDAR are being put to use in an effort to map the entire flood plain of North Carolina, USA, in a flood plain management and risk assesment program. In forestry airborne laser scanning is applied widely, mainly for forest inventory (Ollson, 2004), (Holmgren and Jonsson, 2004).

There are three LiDAR systems that utilises green laser sensors for airborne laser bathymetry. The American Scanning Hydrographic Operational Airborne Lidar Survey (SHOALS) is operated by the Joint Airborne Lidar Bathymetry Technical Center of Expertise (JALBTCX). The Australian Tenix Corporation operates the Laser Airborne Depth Sounder (LADS) and Hawk Eye II is run by Admiralty Coastal Surveys, a joint venture between United Kingdom Hydrographic Office, Airborne Hydrography AB and TopEye AB. Green lasers are more complex and hence, more expensive. The three systems were all launched by government defense institutions. Airborne laser bathymetry has a number of obvious advantages. Where multi beam sounding systems are efficient on deep and medium water, they are less effective in shallow water, because the swaths become too narrow. The width of the laser tracks are unaffected by this, because it is controlled by the flight altitude only. ALB has been carried out in hazardeous areas e.g. shoals and reefs, where ships would be at risk. Other advantages are the high precision, speed of data capture and cost efficiency.
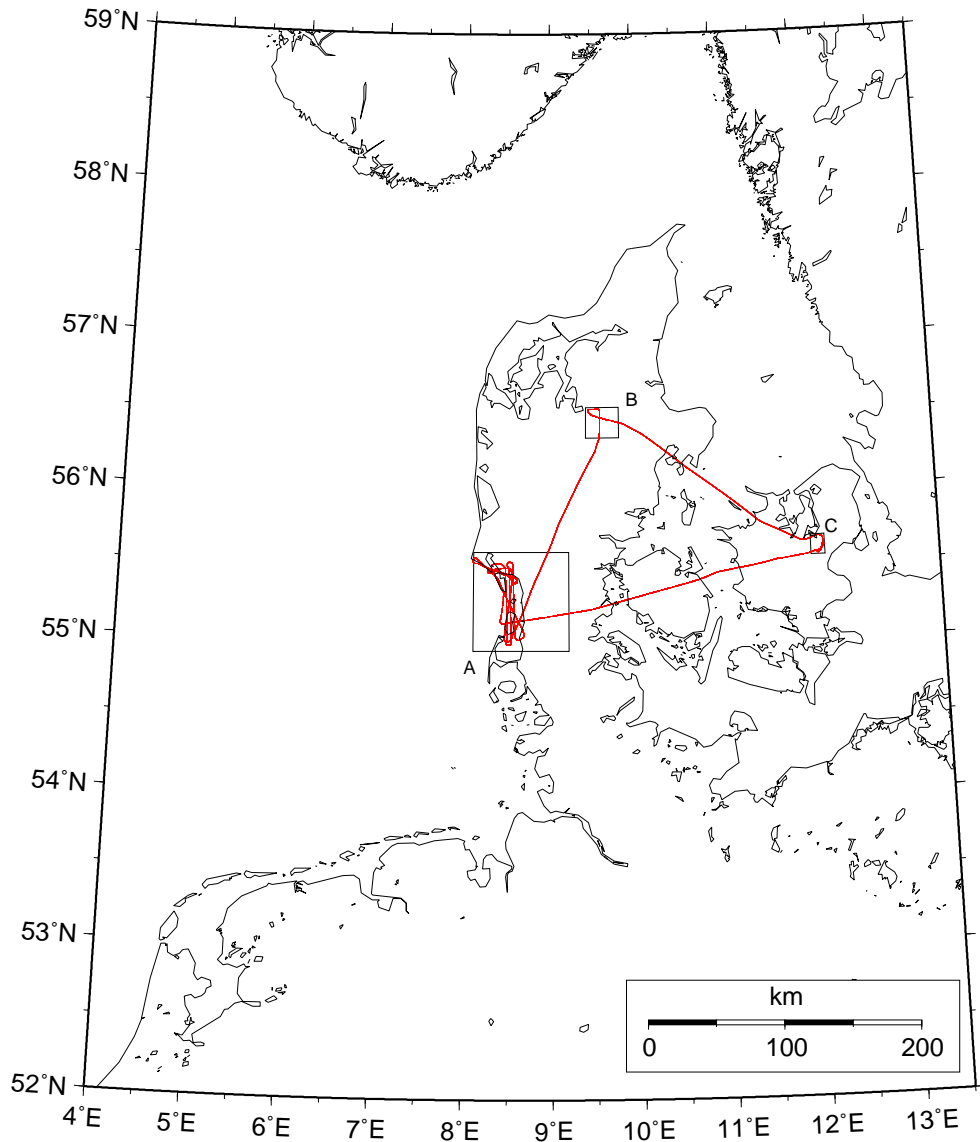
Figure 1.1: *North West Europe. The path of the 2002 Wadden Sea flight is shown in red color. The boxes show were the LiDAR data was obtained. A, B and C are shown in figure 1.2.*
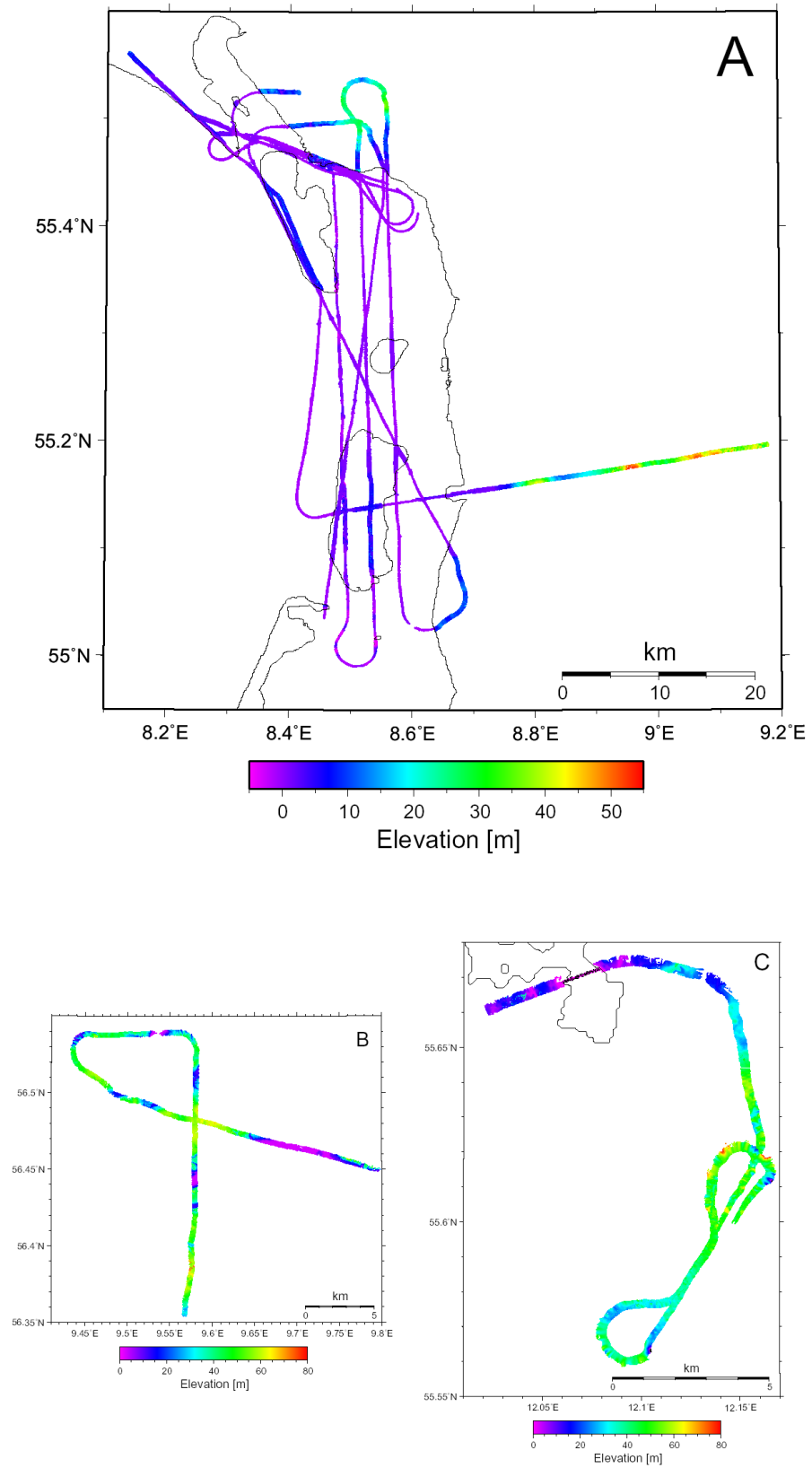
Figure 1.2: *The LiDAR elevation data from the Wadden Sea, A. Data from an area to the north east of Viborg, B and data from Roskilde airport, C.*

Chapter 2

Method

The DNSC airborne LiDAR system consists of three modules: A laser sensor system, a Global Positioning System (GPS) and an Inertial Navigation System (INS). The LiDAR system is mounted on an airborne platform, e.g. a helicopter or more typical, a fixed winged aircraft. A Piper Navajo PA 31 was used for this survey, but the system is flexible and does not require a dedicated platform. The scanning laser rangefinder determines the distance from the laser to an object on the ground. The GPS gives the position of the laser sensor while the INS gives the orientation of the laser. Having determined the laser sensor's position and attitude, the measured laser ranges (r_{ls}) are converted into xyz-triplets, producing a point cloud within a given reference frame.

2.1 Laser

The survey was carried out using the Riegl laser mirror scanner LMS-Q140-60. The laser uses a semiconductor laser diode as laser source. A LiDAR sensor system consists of a laser and a receiver system. The laser generates a 10 ns wide pulse in the near infrared region (905 nm wavelength). The emitted laser pulse is reflected off the ground and the backscatter returns to the system receiver, a photo-diode co-located with the laser. The distance from the laser to the ground (r_{ls}) is calculated by

$$\text{distance } (r_{ls}) = \frac{\text{speed of light} \cdot \text{time of flight}}{2}$$

The laser has a pulse repetition rate (PRR) of 25 kHz. The time of flight is converted into distance using the formula above. The laser pulses are deflected across the flight path by a four-sided polygon spinning mirror. The mirror

Figure 2.1: *The twin piston engine Navajo PA 31 (OY-BHF) that served as platform for the LiDAR system, was chartered from the Danish surveying company, Scankort.*

Parameter	Performance
LiDAR	Riegl LMS-Q140i-60
Total energy of a single laser pulse (nJ)	656
Peak power of a single laser pulse (W)	65.6
Laser pulse freqency (Hz)	25000
Laser wavelength (nm)	905
Scan frequency (Hz)	40
Footprint diameter at nadir (cm)	90
Field of view (degrees)	$\pm\,30°$
Measurement density ($^{hits}/_{m^2}$)	0.4
Beam divergence (mrad)	3
Number of shots per scan	208
Eye safety classification (IEC60825-1:2001)	Class 1

Table 2.1: *Specification of the LiDAR data acquisition. Footprint size and measurement density values assumes operation altitude of 300 m above ground level.*
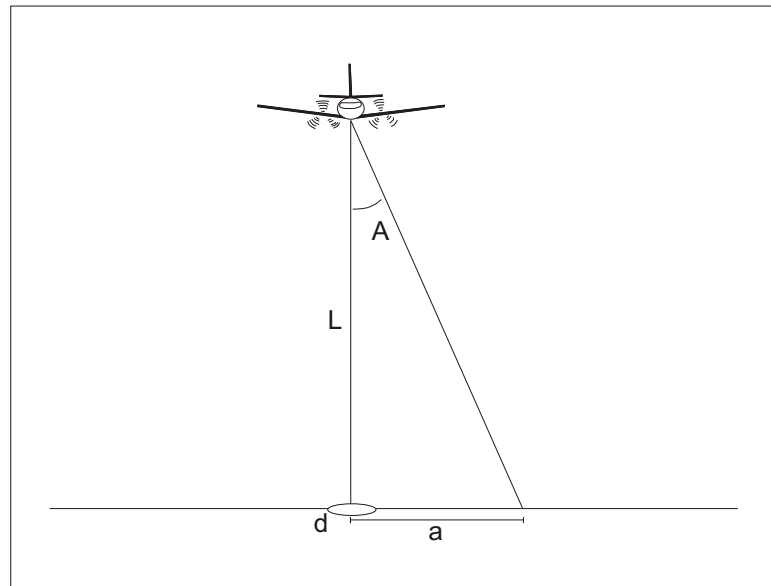

Figure 2.2: *The basic geometrical relations between flight altitude (L), scanning angle (A), swath (2 · a), footprint diameter and beam divergence.*
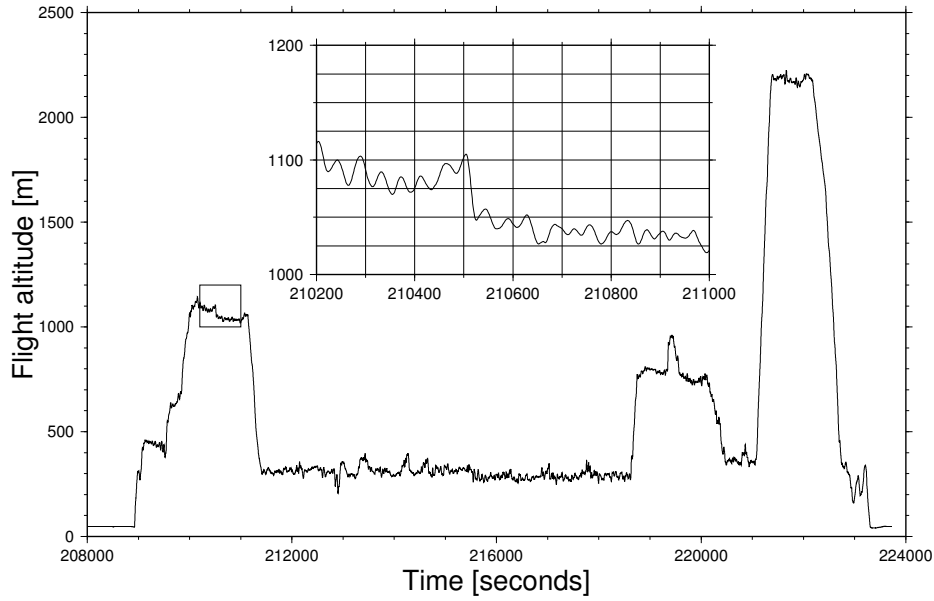
Figure 2.3: *The flight altitude of the survey. Time is UTC seconds and height is in the national height datum DVR90. In the enlarged area is shown the characteristics, (amplitude and period), of the phugoid motion.*

revolves at 40 Hz. The total energy of a single laser pulse is approximated

$$E_{total} = \frac{P_{average}}{PRR} = \frac{16.4 \cdot 10^{-3}\,\text{W}}{25\,000\,\text{Hz}} = 656\,\text{nJ}$$

The value for $P_{average}$ is provided by Riegl. The peak power of a single laser pulse is calculated by

$$P_{peak} = \frac{E}{t} = \frac{656\,\text{nJ}}{10 \cdot 10^{-9}} = 65.6\,\text{Watt}$$

The width of the scanned laser swath in the terrain is controlled by the flight altitude and the scan angle of the laser. The footprint size depends on the altitude and the laser beam divergence. The Riegl laser has a scan angle of $\pm 30°$ and a beam divergence (α) of 3 mrad. The swath width can be calculated by

$$\text{swath width} = 2 \cdot a = 2 \cdot L \cdot tan(A) = 2 \cdot 300\,\text{m} \cdot tan(30°) \approx 346\,\text{m}$$

while the nadir footprint diameter (d) is given

$$\text{diameter} = L \cdot sin(\alpha) = 300\,\text{m} \cdot sin(0.003) = 0.90\,\text{m}$$

The relationship between flight altitude, footprint and swath is shown on figure 2.2. The size of the nadir footprint increases 30 cm per 100 m altitude. Operating approximately 300 m above ground level, with an airspeed of roughly 100 m/s, the laser produces a 350 m wide swath. The footprint diameter is 90 cm and the point density is 1.5 m along-track, as well as across-track (assuming no acceleration). The laser scanner records the last significant return. The last significant return is most likely to represent the ground return. This reduces the amount of data that is captured and has to be stored. As a consequence the data is not well suited for classification purposes, which usually uses full wave sampled data. No algorithms have been implemented to obtain bare-earth models or auto detection of houses, etc.

11

2.2 GPS

Two separate geodetic dual-frequenzy GPS receivers were used to determine position of the aircraft antenna. A Trimble 4000 SSI and a Javad Legacy both shared the same antenna and recorded at 1 Hz. Differential GPS solutions were post-processed using two reference sites, the permanent geodetic stations at Buddinge and Smidstrup (table 2.2). The precise IGS orbits (ephemeris) were obtained from (ftp://cddisa.gsfc.nasa.gov/pub/gps/products/). Solutions were computed with the commercial kinematic GPS software GPSurvey (version 2.35), developed by Trimble, using OTF ambiguity resolution techniques. Different constellations of GPS receiver and reference station were computed. In the end a solution using the Javad Legacy and Buddinge reference station was chosen. In general, good agreement existed between solutions, typically less than 5 cm.

2.3 INS

In order to determine the direction of the laser beam, the orientation of the laser sensor must be determined. This is done with the Inertial Navigation System (INS). The INS consists of a hardware part, the Inertial Measurement Unit (IMU), measuring rotation velocities and accelerations, and a software part converting them into attitude, position and velocities within a chosen reference system. The INS used was the H-764G embedded GPS/INS (EGI), a medium grade strap-down system developed for military use, by the American company Honeywell. The IMU consists of three ring laser gyros, three QA2000 accelerometers, a temperature sensor and matching electronics. Because of the embedded GPS, navigation solutions employ GPS/INS integration. This has a number of advantages. It is possible to achieve stronger navigation solutions, two independent data sources are used, INS gives position when GPS fails (cycle slips) and most importantly, the GPS constrains the INS positions.

Both free inertial and Kalman filtered GPS-integrated position and attitude data were logged at 50 Hz on a laptop PC in binary format through a 1553 milspec. communications bus to the output file: egi-020305-105003.dkk, following the typical naming convention (year/UTC-time) YYMMDD–HHMMSS.dkk. This file was reformatted to 10 Hz using the software READEGI, producing the ascii file: readegi.coo. The file contains

$$thr \quad lat \quad lon \quad h_{GPS} \quad pitch \quad roll \quad heading \quad h_{int}$$

where thr is the UTC-time in decimal hour. The position of the GPS-antenna is given in WGS84. The ellipsoid height of the antenna is recorded by h_{GPS}, the value given by the embedded GPS. The last column of the file records the integrated height of the antenna (h_{int}) calculated from the velocities provided by the accelerometer, (h_{int}) has a higher internal short-term accuracy than h_{GPS}. The attitude data (roll, pitch and heading) are given in degrees and are defined in the aircraft body coordinate system ($\mathcal{B}$). This is a cartesian right-hand coordinate system with the 1. axis is in the flight direction. The 2. axis points

Station	ID	Latitude	Longitude	Elevation
Buddinge	1-13-829	55° 44′ 20.46011″	12° 30′ 0.07098″	94.015 m.
Smidstrup	117-05-810	55° 38′ 26.31332″	9° 33′ 33.48734″	122.794 m.

Table 2.2: *Reference stations in EUREF89/REFDK systems. Elevation is ellipsoid height.*

to the right in the direction of the wing and the 3. axis points down toward the floor of the aircraft. The origin of the system is in the INS. Pitch increases as the nose of the aircraft pulls up. Heading is positive towards the right and roll increases when aircraft turns right (and the left wing tip is up).

The next step was merging the GPS file and the INS file. This was done with GPSEGI, a program to patch voids and interpolate GPS solutions by draped INS data, producing the ascii file gpsegi.pos, containing

> *thr   lat   lon   h   pitch   roll   heading*

Both position and height values are corrected using the INS data.

2.4   Processing Laser Data

The Riegl laser scanner logs output through an ecp parallel port to a laptop computer while a RS232 serial port is used for commands. The laser produces 25 000 pulses every second (this is user-selectable). An internal quartz stabilized timer, counting with a frequency of 100 kHz, puts a time tag on every pulse return measurement. The timer is reset by the external 1pps pulse from the GPS receiver. Files are named after the time they are started. Filenames, locations, start and stop times are given in table 2.3.

The logging system of the Riegl laser scanner does not allow for the recording of integer seconds. As a result of this there is a risk of lack of syncronization between the laser and the GPS/INS, and caution is required when merging the files. An integer second off-set results in translations at multiples of approximately 100 m on the ground, (the distance travelled in one second). When the laser ranges and attitude data are mismatched, the resulting terrain model will have an undulating (rolling) appearance. This is easily corrected but emphasizes the importance of the air log (appendix A).

The final processing of the laser data was done with READSCAN (version 1.2). READSCAN recovered the GPS-time, laser mirror angle α and the measured range r, from the raw binary scanner files. These were then combined with interpolated values for coordinates and attitudes from the gpsegi.pos output-file.

In order to obtain ground elevations in the desired reference system it is necessary to transform observations from one system to another. A transformation consists of a rotation and a translation when the two coordinate systems do not share the same origin. Assuming that two coordinate systems share the same origin, but have a different orientation, one system can be projected into the

Filename	Start (dec. hour)	Stop (dec. hour)
104400.2dd	10.7300	11.1105
111000.2dd	11.1670	11.6200
114000.2dd	11.6660	12.7505
131300.2dd	13.2160	13.4205
135200.2dd	13.8660	14.0500

Table 2.3: *List of Riegl raw scanner data files. The time intervals are given in decimal hour, UTC-time.*

other by three consecutive rotations around the coordinate axes. $R_1(\phi)$ is the rotation by the roll angle ϕ around the 1. axis, while $R_2(\theta)$ is the rotation by the pitch angle θ around the 2. axis and $R_3(\psi)$ is the rotation by the heading angle ψ around the 3. axis. The three rotation angles are called Euler angles and the rotation matrices are

$$R_1(\phi) = \begin{pmatrix} 1 & 0 & 0 \\ 0 & cos\phi & sin\phi \\ 0 & -sin\phi & cos\phi \end{pmatrix} \qquad R_2(\theta) = \begin{pmatrix} cos\theta & 0 & -sin\theta \\ 0 & 1 & 0 \\ sin\theta & 0 & cos\theta \end{pmatrix}$$

$$R_3(\psi) = \begin{pmatrix} cos\psi & sin\psi & 0 \\ -sin\psi & cos\psi & 0 \\ 0 & 0 & 1 \end{pmatrix}$$

The three rotations combines to form the full attitude matrix

$$
\begin{aligned}
R_A^B &= R_1(\phi)R_2(\theta)R_3(\psi) \\[2mm]
&= \begin{pmatrix} 1 & 0 & 0 \\ 0 & cos\phi & sin\phi \\ 0 & -sin\phi & cos\phi \end{pmatrix} \begin{pmatrix} cos\theta & 0 & -sin\theta \\ 0 & 1 & 0 \\ sin\theta & 0 & cos\theta \end{pmatrix} \begin{pmatrix} cos\psi & sin\psi & 0 \\ -sin\psi & cos\psi & 0 \\ 0 & 0 & 1 \end{pmatrix} \\[2mm]
&= \begin{pmatrix} cos\theta cos\psi & cos\theta sin\psi & -sin\theta \\ sin\phi sin\theta cos\psi - cos\phi sin\psi & sin\phi sin\theta sin\psi + cos\phi cos\psi & sin\phi cos\theta \\ cos\phi sin\theta cos\psi + sin\phi sin\psi & cos\phi sin\theta sin\psi - sin\phi cos\psi & cos\phi cos\theta \end{pmatrix}
\end{aligned}
$$

R_A^B is the rotation matrix from system A to system B.

The observed laser ranges are defined in the laser body system ($\mathcal{S}$). This has the same origin as the aircraft body system $\mathcal{B}$, but the axes are slightly off-set because it is impossible to orientate the laser perfectly to the INS body system. This is called the boresight misalignment and remains constant as the laser and INS system are rigidly mounted in the aircraft. The typical procedure in order to obtain these off-set angles is to fly a cross or preferably a four leaf clover signature over a known GPS-positioned object, usually buildings. The firestation at Roskilde airport was used for this purpose. The off-set values were found to be

$$\phi_0 = 0.06° \qquad \theta_0 = 0.66° \qquad \psi_0 = \text{-}0.51°$$

With the boresight misalignment established, the observations are transformed from the laser body system $\mathcal{S}$ to the INS body system $\mathcal{B}$ by the rotation matrix $R_{\mathcal{S}}^{\mathcal{B}}$.

Next the observations are transformed to the local level coordinate system ($\mathcal{L}$), also called a NED-system (North East Down). In this system the 1. axis is parallel to the tangent to the ellipsoid pointing to the north. The 2. axis is also parallel to the tangent to the ellipsoid but pointing to the east. The 3. axis is the normal to the plane spanned by the 1. and 2. axis, pointing downwards. The origin of the system is in the GPS antenna and the antenna off-set given by $\Delta x, \Delta y, \Delta z$. The off-set between the GPS antenna and the laser was measured and the antenna off-sets were found to be

$$\Delta x = 0.0 \text{ m} \qquad \Delta y = -0.35 \text{ m} \qquad \Delta z = 1.42 \text{ m}$$

Applying 3-dimensional geometry the laser ranges (r_{ls}) are turned into ground elevations using:

$$
\begin{bmatrix} \varphi \\ \lambda \\ h \end{bmatrix}^{GP} = \begin{bmatrix} \varphi \\ \lambda \\ h \end{bmatrix}^{GPS} + R^{\mathcal{L}}_{\mathcal{B}} \begin{pmatrix} \phi \\ \theta \\ \psi \end{pmatrix} \left[\begin{bmatrix} \Delta x \\ \Delta y \\ \Delta z \end{bmatrix} + R^{\mathcal{B}}_{\mathcal{S}} \begin{pmatrix} \phi_0 \\ \theta_0 \\ \psi_0 \end{pmatrix} r_{ls} \right]
$$

READSCAN produces 2 output files. The scanner file (.scn file) contains all georeferenced elevations. It also records the intensity of the returned laser pulses and their scan no. Besides being time tagged, each measured return is given a scan number between 1-208 (first and last shot in the line scan). The intensity of the returned laser pulse is measured and given as an index of the energy of the emitted laser pulse, with range 0-255. In READSCAN a lowest threshold was set to 10. Returned laser pulses with an index value lower than 10 were discarded. This was done in order to avoid *noise* in the data. The READSCAN basic scanner output file contains

    thr   *lat*   *lon* h_{GP} *intensity*   *scan no.*

The vertical (.ver file) file has only one measurement per line scan, the central point in a swath. The vertical file records the track under the airplane. If the airplane rolls left the track is displaced to the right. The vertical file contains the data

    thr   *lat*   *lon* h_{GP} *intensity* h_{GPS} r_{ls}

where r_{ls} is the measured laser range. The Danish national geoid model DK-GEOID02 (accurate to 1-2 cm) were used to convert heights from the GPS ellipsoid system to the the Danish height system DVR90.
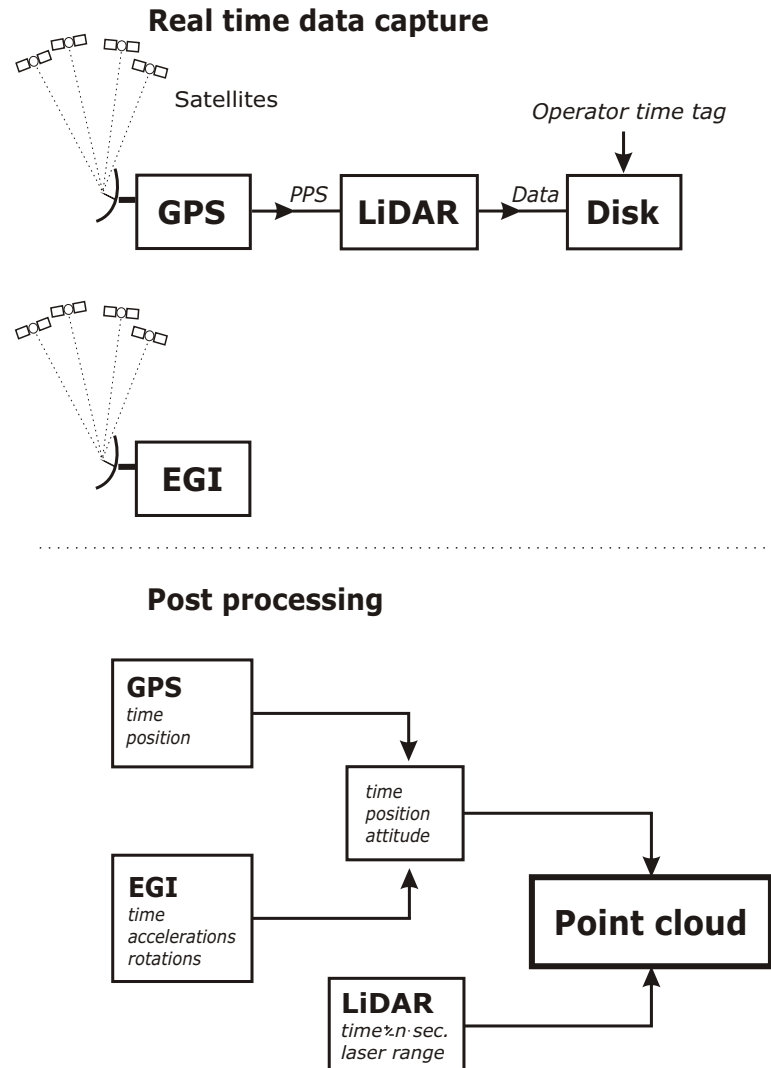
Real time data capture

Post processing

Figure 2.4: *Data flow diagram of the LiDAR system. EGI is a medium-grade Honey-well GPS-integrated inertial navigation system (H764G), providing aircraft attitude. Because the data generated by the GPS and the EGI are time-tagged using the same satellites, position and attitude data are perfectly synchronised. The LiDAR sensor uses an internal high speed timer (100 kHz) to time-tag pulse returns. The timer is reset every second by the PPS pulse from a GPS receiver. The Riegl logging system does not allow the recording of integer seconds, so the scanner file is time-tagged by the the operator. The precise time (integer seconds) must be recorded, otherwise the syncronization between the GPS/EGI and the laser data is erronous, corresponding to multiples of approximately 100 m on the ground. A lack of syncronization between the attitude and the laser data, gives the terrain model an undulating appearance, and is usually easily identified.*

Chapter 3

Results

Five laser scanner files were processed and transformed into elevations. The total amount of data consists of 20,599,832 georeferenced elevations in 329,334 scan lines. Because of the large amount of data, scanner files are typically processed in 2 minute segments thus making handling and visualization more manageable. The entire dataset is displayed on figure 1.2. Below are given a few examples of the quality of the LiDAR DEM. From the examples it is clear that houses and building structures are clearly identified. Even if the point density is lower than required for technical urban DEMs, the building structures are well defined (figure 3.2 and figure 3.3), even cars can be identified from the data. Some rooftops are non-reflective. Roads are often non-reflective but it is not uncommon that the white road stripes give a reflection. Roads are often more effectively identified from the intensity data layer (figure 3.1).

Some types of vegetation has very little reflection. This is evident on figure 3.6 on the western side of Rømø, while the laser strip crossing Mandø has good coverage. It is possible that there was no vegetation in the early spring, thus making it a bare-earth model.

The reflection pattern on the beach face seems to be controlled by water, dry sand reflects well while wet sand reflects less, if at all. Water has the special characteristic like a mirror, reflecting the laser beam away from the receiver. Only the laser shots directly under aircraft (nadir) are reflected back to the receiver. These however have high intensities. There is a narrowing of the laser strip in front of the beach cliff. When viewing the intensity data it is concluded that this records the position of a water-filled beach furrow.
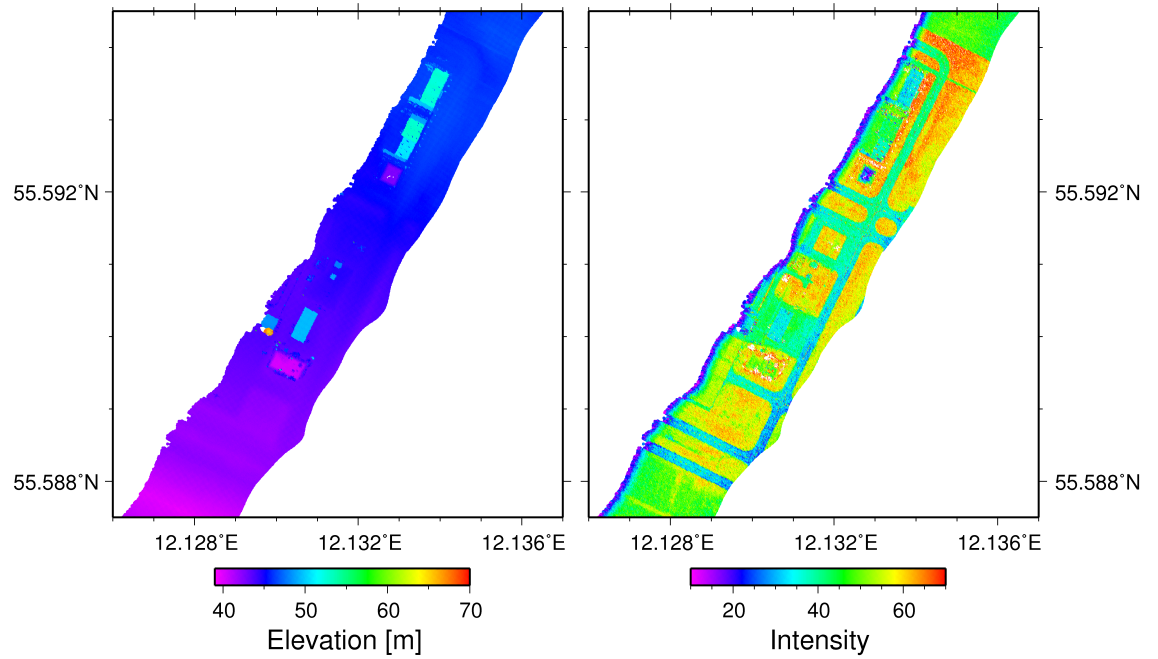
Figure 3.1: *The laser strip across Roskilde airport. The elevation data is displayed to the left while the intensity is shown on the right side. The flight direction is towards south-west. It seems that the return intensities are systematically smaller to the far right of the scan. This phenomenom is also seen on figure 3.5.*
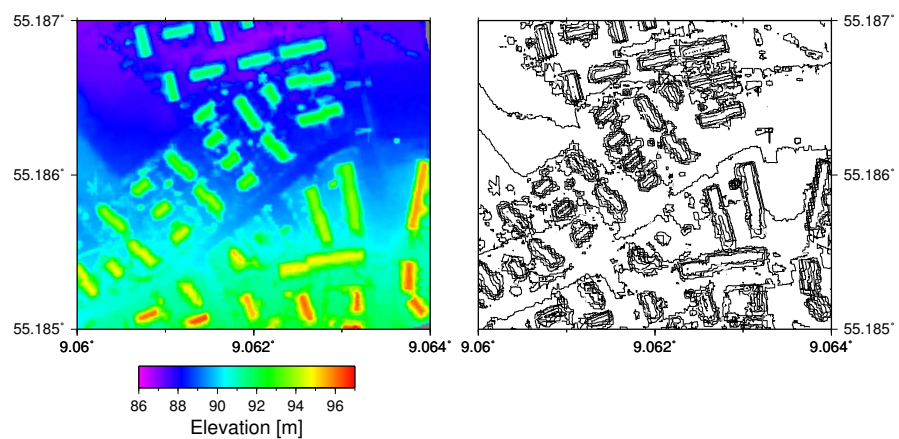

Figure 3.2: *The LiDAR derived DEM from the town of Toftlund, an urban area in the south of Jutland, to the left. On the right is shown a contour plot of the same area with 1 m contour lines.*
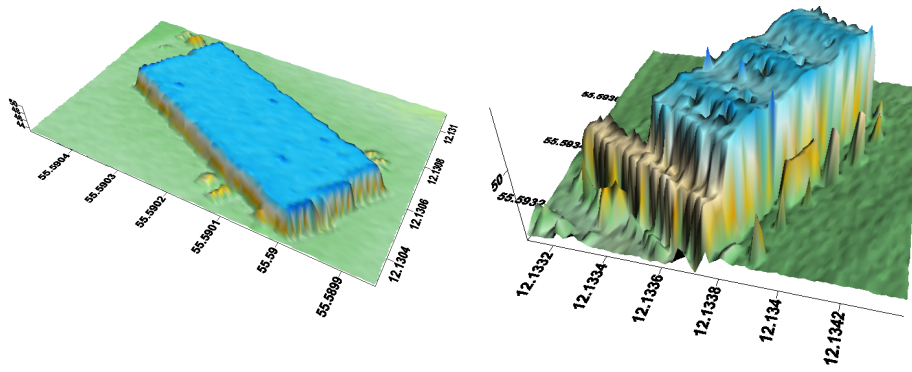
Figure 3.3: *Two false colour examples from Roskilde airport. On the left is the firestation used for calibrating the boresight misalignment, while one of the terminal buildings are shown with the vertical scale exaggerated, to the right. Note the arched roof and what appears to be trees or light masts in front of the building.*
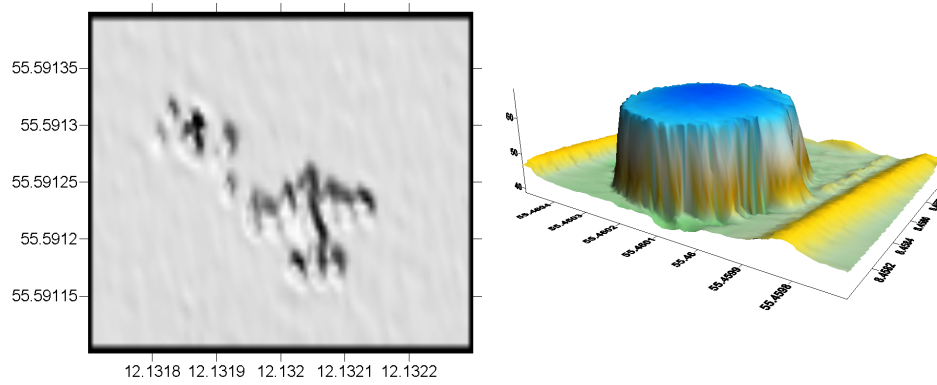

Figure 3.4: *Left: An aircraft from Roskilde airport displayed in shaded relief. Right: A tank structure from Esbjerg is shown in false colour.*
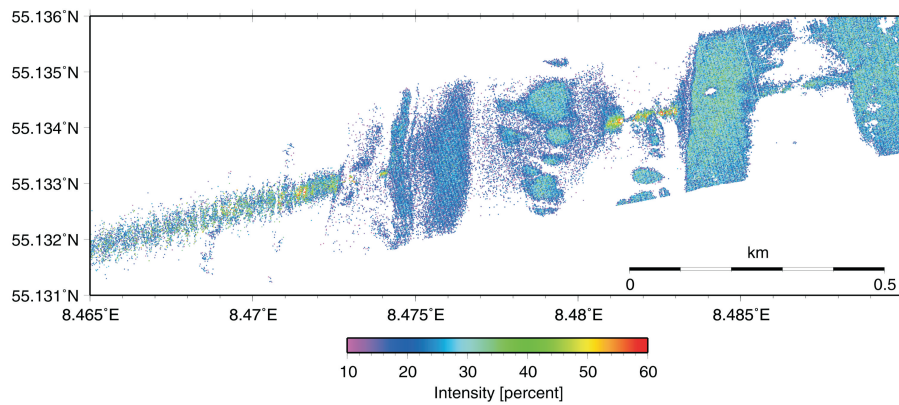

Figure 3.5: *The beach face on the western side of the Danish island Rømø. The distribution and intensity of the reflected laser pulses indicate the position of a beach furrow on the back beach.*
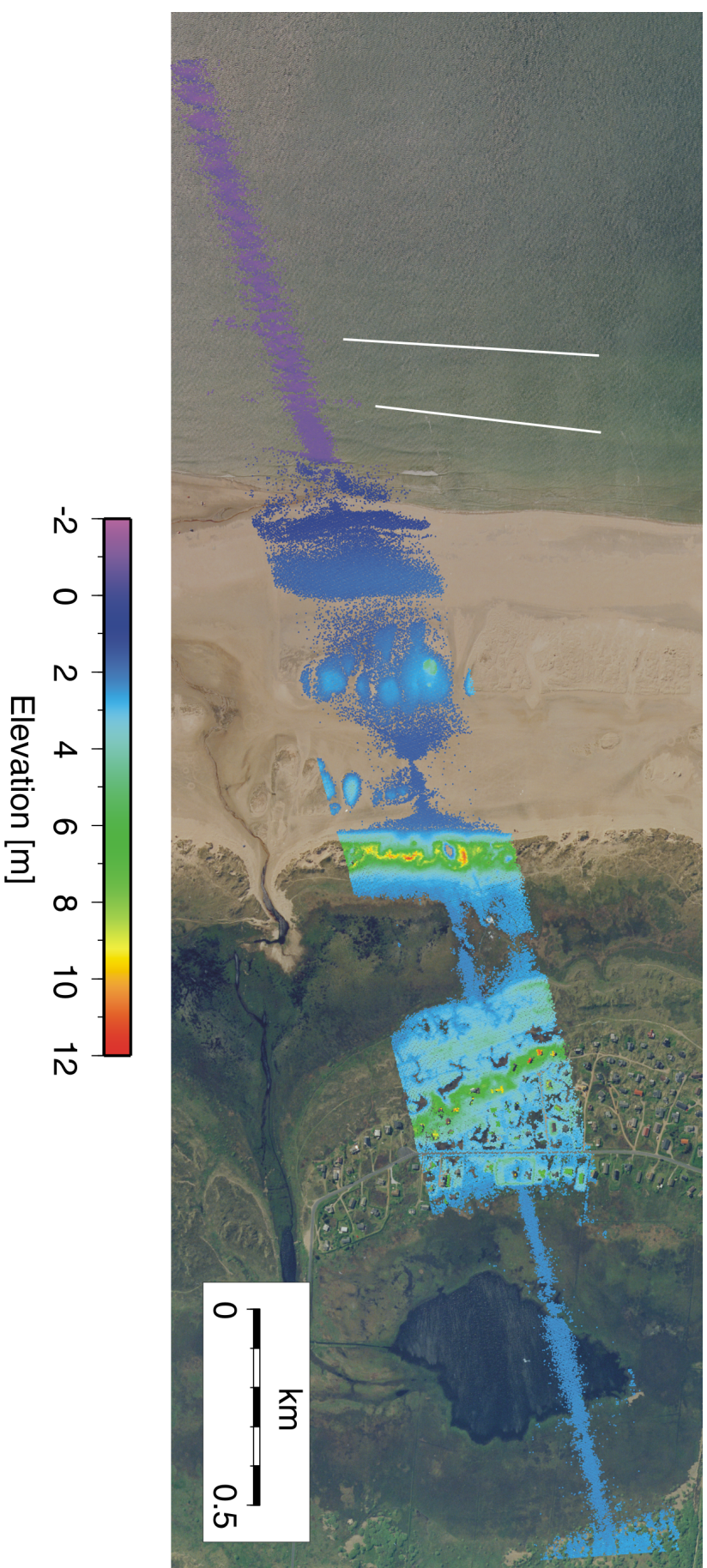
19

Figure 3.6: *The scanned track over the western part of Rømø. The vegetation in the wetlands only reflect near-nadir laser signals. Some houses are very clearly shown while other rooftops are non-reflective. The white lines indicate the position of two longshore bars. The waves break over the bars in the break zone, creating a wider reflection than over calm water. The photograph, that was taken two years prior to the laser scan, belongs to National Survey & Cadastre (Kort & Matrikelstyrelsen) annual aerial photo series, Project 2000-08.*
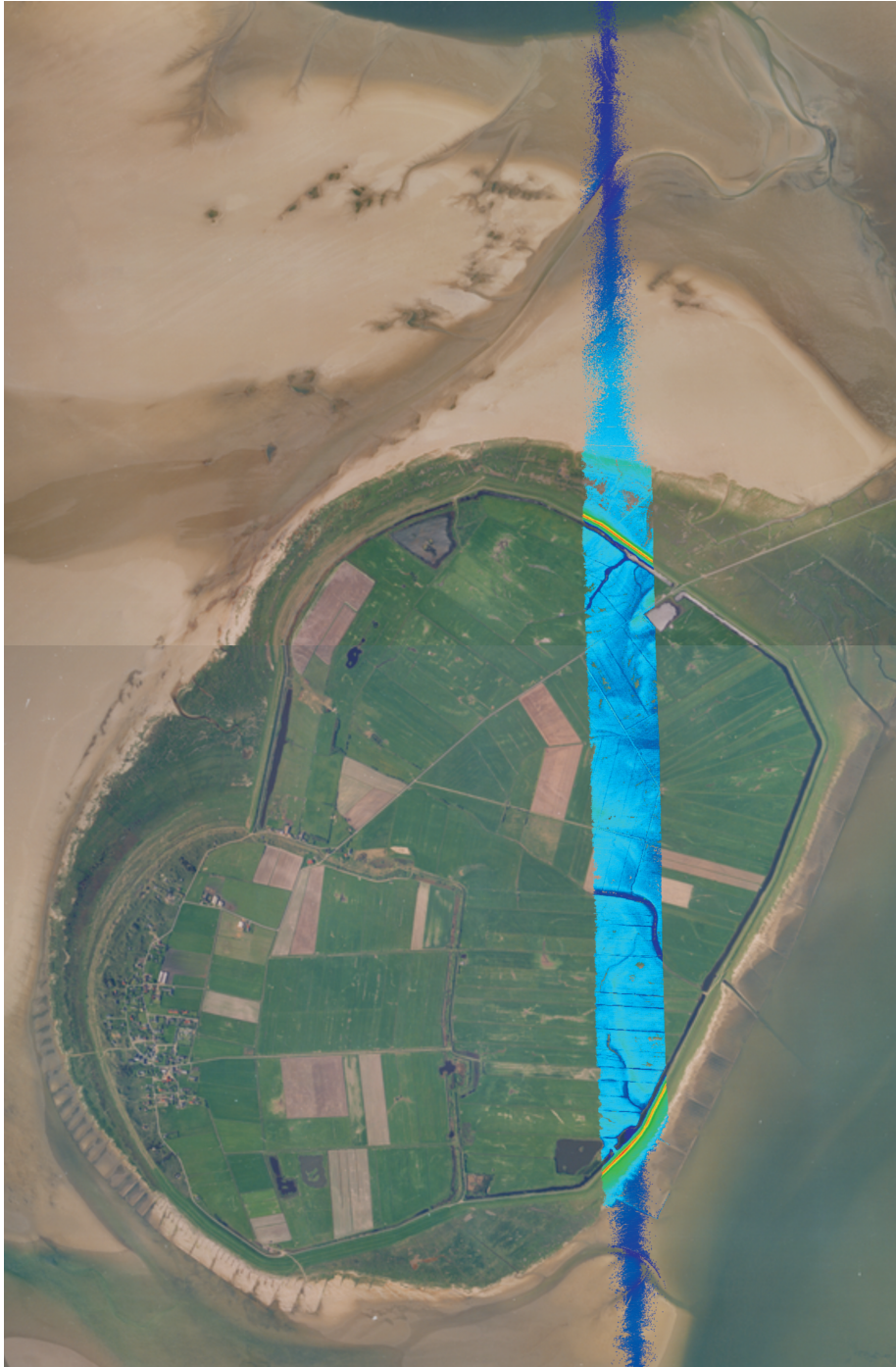
20

Figure 3.7: *The laser strip crossing the island of Mandø. The photograph was taken two years before the laser scan and belongs to the National Survey & Cadastres annual aerial photo series, Project 2000-08.*

Chapter 4

Validation

In general, the precision of the heights obtained from laser scanning is affected by the precision of the hardware: the laser, the GPS and the INS. The quality of the laser depends on the precision of the travel time measurement (clock), and the precision and regularity of the spinning mirror. The GPS is influenced by ionospheric and atmospheric delay, cycle slips and loss-of-lock, for instance when the airplane makes a turn. Errors in GPS solution are systematic and directly transferred to laser groundpoints. Inaccuracies in the rotations of the gyroscopes and accelerometers of the INS causes errors in the rotation angles given by the INS. The surface type also affects precision. The laser produces a foot print on the ground. Because this is an area, rather than a point, it can cover different objects, having different elevations. The measured laser range is the discrete peak of the return signal. A laser pulse that hits a sloping surface can also give a faulty range. Finally the accuracy of the calculated bore-sight misalignment and antenna off-sets will influence the overall quality of the point cloud.

In this survey different approaches was made to obtain ground truth and validate the quality of the scanned height model. First all referenced geodetic benchmark fix points from the Wadden Sea region were collected. Attempts were made to compare these to the LiDAR elevations. Unfortunately they were generally too far away from any LiDAR elevations to be used. In Esbjerg harbour a number of fix points were situated within a laser strip however. Because fix points typically are placed on buildings, it proved impossible to use them to validate the LiDAR model.

Where different tracks cross, a fast collocation interpolation estimator, (GEO-GRID), was used to evaluate the height difference between the data sets, thus giving a measure of the self-consistency of the method. The crosses that were analysed showed little discrepancy between measured elevations. The mean difference between tracks were typically less than 15 cm, with standard deviation less than 5 cm. The mean difference is interpreted as the uncertainty of the GPS solution while standard deviation is believed to represent the noise-level of the data. The main discrepancies between height models are tied to vegetation, e.g. trees. This is because a tree will show different elevations depending on the penetration of the laser pulse (figure 4.1). The difficulties of determining true canopy height are adressed by Hyyppä et al. (2004).

>From a number of locations in the survey area, a series of GPS measurements were collected using a Trimble 4000 SSI GPS receiver. With the antenna mounted on the roof of a car, data was collected from Rømø, Rømø-dam, Jutland and the coastal road to Mandø. The Mandø data does not overlap any LiDAR data and will not be discussed further. Data was also collected from a pier at Esbjerg
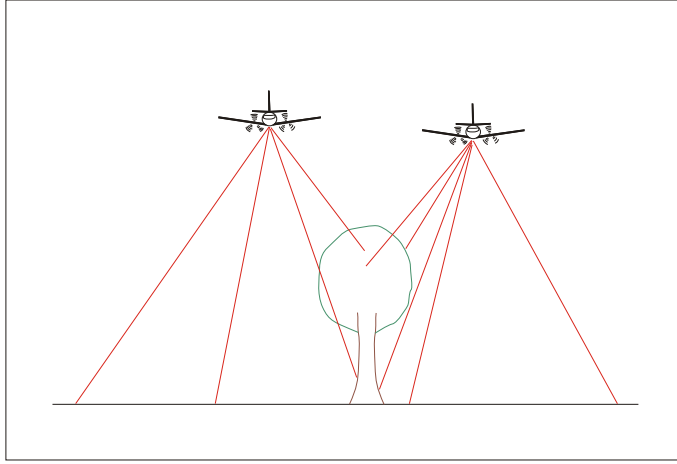
Figure 4.1: *Vegetation are not readily compaired because of the lack of vertical control and different penetration.*

harbour and from a profile section across the Rømø dam. Again the Trimble 4000 SSI was used with the GPS antenna mounted on a rod and moved around by foot (figure 4.2). The antenna off-sets were

$$\Delta z_{car} = 1.74 \text{ m} \quad \Delta z_{rod} = 2.06 \text{ m}$$

The GPS solutions that were made all used Buddinge as reference station but only 15-second data was available for the profile across the Rømø dam and Esbjerg harbour. The GPS data that were collected was compared with the LiDAR data, using GEOGRID, and the results are shown in table 4.1. The GPS elevations obtained from the roof-mounted setup shows stronger correlation with the LiDAR data than the elevations obtained from Esbjerg harbour and Rømø dam. The reason for this is probably that flat surfaces e.g. roads and runways are very suitable for providing ground truth. Elevations from the edge of the pier at Esbjerg harbour can be compared to points on the side of the pier, because of their close proximity, i.e. there is weak spatial control around vertical structures. It is not clear why the Rømø dam cross profile and LiDAR data shows weak correlation, but it seems that the problem lies with the GPS elevations across the Rømø dam. The data collected by the roof-mounted GPS shows excellent correlation with the LiDAR data. The difference between the two data sets are displayed on figure 4.3. The outliers can be identified as cars and in one case a truck with a trailer. Eliminating the outliers, the mean difference (bias) between the data sets is 2 cm and the standard deviation (noise) is 8 cm. This is a very good result for kinematic GPS, considering the baseline length to the Buddinge reference GPS station is more than 200 km.

File	Location	mean diff.	std. dev.
22030641.dat	Rømø dam road	0.02 m	0.08 m
22030642.dat	Mandø coast road	N/A	N/A
22030643.dat	Esbjerg harbour	0.24 m	0.10 m
22030644.dat	Rømø dam profile	0.62 m	0.28 m

Table 4.1: *The difference in heights between the LiDAR derived elevation model and the field measured elevations.*

Figure 4.2:   *To validate the DEM, GPS control points were collected. This was done with a roof-mounted antenna on a car (left) and by moving the antenna around Esbjerg harbour by foot (right).*
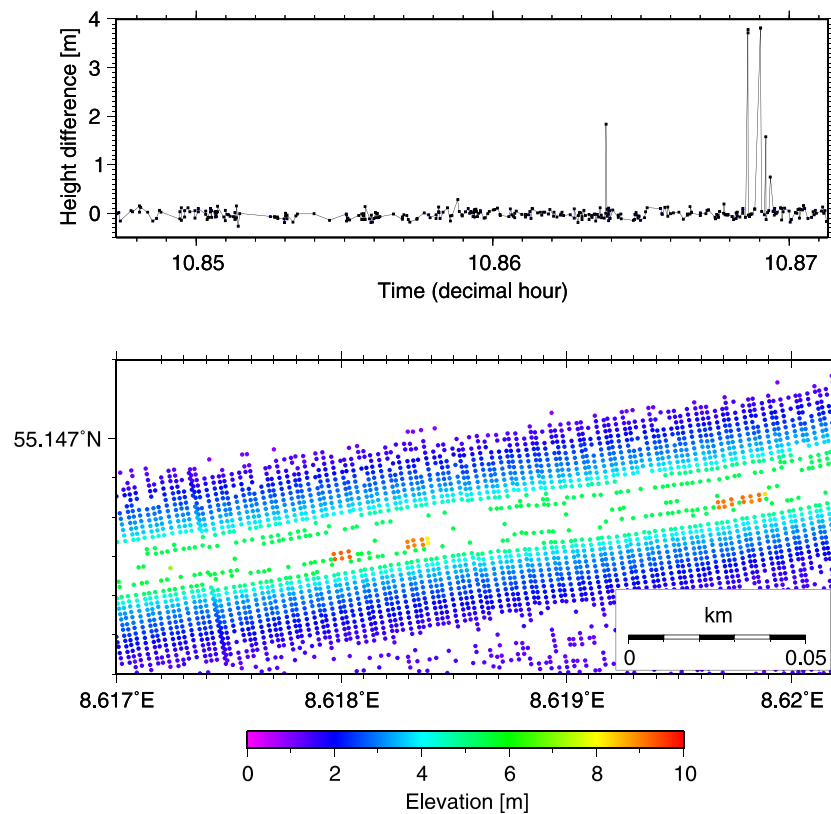

Figure 4.3:   *In order to obtain validation, the LiDAR elevation data from the Rømø dam road was compared with the data collected with the roof-mounted GPS antenna. Comparison was done whenever a data point from one data set was within 1 m of a data point from the other data set. The upper panel shows the difference in elevation between the two data sets as a function of time, where the time refers to the airborne laser scanner data time tags. With the exception of a few outliers the consistency of the data sets are excellent. After examining the laser scan (lower panel), the outliers are identified as vehicles. Cars and trucks will appear on the laser scan but for obvious reasons, not in the roof-mounted GPS data.*

Site	LiDAR survey 1	LiDAR survey 2	Ground truth	TOP10DK
Terminal	48.40 ± 0.10 m	48.32 ± 0.09 m	48.33 ± 0.05 m	48.80 ± 0.70 m
Firestation	49.58 ± 0.05 m	49.44 ± 0.05 m	49.62 ± 0.05 m	49.70 ± 0.70 m
Tower	67.85 ± 0.30 m	67.43 ± 0.21 m	N/A	68.06 ± 0.70 m

Table 4.2: *Comparison of heights from airborne laser scanner, ground truth GPS survey and the digital map TOP10DK of KMS. 3 different buildings in Roskilde airport. LiDAR survey 1 is the present survey while LiDAR survey 2 was carried out on 2001-07-27 and described by Arens (2002).*

In Roskilde airport a comparison was made between different measurements of roof elevation from the firestation, terminal building and the tower. LiDAR elevations exist from an earlier survey flight. These were compared to measurements taken in the field by traditional surveying and data from the TOP10-DK topographic database. The results are shown in table 4.2. The present survey is denoted LiDAR survey 1. The LiDAR heights are within approximately 10-15 cm of each other. This is probably the inaccuracy of the GPS solution. The noise given by the standard error is small, i.e. 5-10 cm. The LiDAR results are within the inaccuracy given by TOP10DK. TOP10DK records the height of the roof's gutter by photogrametry. Less weight is put on the measurements of the tower because the concave shape of the roof makes it unsuitable for comparison purposes. It is concluded that the accuracy of the LiDAR derived elevations is satisfactory, and likely around 10 cm.

Chapter 5

Conclusion

Five laser scanner files have been processed and turned into approximately 20.6 million georeferenced elevations. The bulk of the data were from the Danish Wadden Sea region. Laser scanner data was also recorded from an area north east of Viborg and from Roskilde airport. The data was processed using the software: READEGI, GPSEGI and READSCAN, all developed by the DNSC. The GPS solution was made with Trimble's GPSurvey. For validation and comparison, GEOGRID, part of the DNSC Gravsoft package developed for geodetic modelling was used.

The laser data show good overall coverage. Some surfaces do not reflect the laser signal. This is true for roads, some roof types and certain types of vegetation. It seems that dry sand reflects the laser signal well. The lack of signal on part of the beach is caused by water. The partially missing signal, also observed on the beach face, is belived to reflect sedimentary bedforms that are partially covered by water. Alternatively it could reflect the level of water saturation. When looking at the distribution and intensity of the laser data from the beach face, different beach elements can be seen: The position of a beach furrow and two coastal bars are identified. We believe that coverage could be increased with lower flight altitude. The data density is 0.4 points per m^2. In this resolution houses and even vehicles can be identified.

Attempts to validate the LiDAR data was made and the results were satisfactory. The precision of the data is on the dm level and the main error source appears to be the kinematic GPS positioning.

The LiDAR system used is owned and operated by the Danish National Space Center (DNSC). It is a relatively low cost system comprising three modules: A GPS, an INS and a laser scanner, at a combined cost of only a small fraction of commercial LiDAR survey systems.

The Wadden Sea region survey demonstrates the major advantages of airborne laser scanning: High precision, high point density, high speed data capture, flexibility and cost efficiency. We believe that repeated LiDAR surveys would be useful for beach mapping and change detection analysis along the Danish coastline.

Chapter 6

Future Work

Airborne LiDAR technology has proved to be a powerful tool in an increasing number of fields. Due to the advantages of speed, precision and cost efficiency, the method is likely to propagate into new fields where reliable 3-D models are desired. One data layer that isn't yet fully integrated is the intensity. Terrestrial laser scanners are able to reveal water leakage on tunnel walls, by using the intensity signal. Roads are likewise readily distinguished from the intensity data. Still, a fully comprehensive method of integrating intensity has yet to be implemented.

In order to spread the use of LiDAR it is important to reduce the cost of the systems. The quality and precision of the data produced are sufficiently high for most purposes. The drive for ever increasing accuracy could serve as a bottle-neck impeding commercial use of the technology. The DNSC modular approach ensures a high quality system at only a fraction of the normal cost.

In coastal areas there are a number of potential uses for LiDAR. The Dutch approach of mapping the entire beach plain every year gives a unique possibility to make change detection analysis and monitor coastal change. In Denmark it is also of great importance to be able to reliably quantify erosion and deposition along the west coast and in the inlets to the Wadden sea. The entire beach plain along the west coast of Denmark could be surveyed in days.

Finally it would be interesting to perform an airborne laser bathymetry (ALB) survey to tie sea topography and surface topography together. In the Netherlands this has been attempted when an area measured at low tide with airborne laser scanning (ALS), is echo sounded at high tide. Observations has shown a discrepancy between LiDAR and echo sounding data, without determining the reason for the actual error though (Vosselman, pers comm).

Acknowledgements

Appendix A

Airborne Altimetry Log

Wadden Sea 5/3 2002
Julian day 64
GPS week 1156 (day 2)

hhmmss		hhmmss	
094500	instrument start-up	113900	new scanner file
	taxi to apron	113900	file is closed
100000	start INS, align		
100100	new scanner file	113959	new scanner file "114000.2dd"
100200	start taxi		line C-D
100330	take-off	114230	sand/water, good data
101100	scanner file closed	115000	eol
101800	The Great Belt, clouds		150 knots, 900 ft.
102200	new scanner file "test2.2dd"	115330	line F-E
	closed, OK		line G-H
		121100	Mandø
104358	new scanner file "104400.2dd"	121300	Rømø
	150 knots, 1000 ft.	121400	dam
	clouds	121630	eol
	starting line N-M		Esbjerg town
105300	Rømø dam		transport line south
105440	eol (end of line)		line Æ-Z
	transport line	124500	eol
105930	Fanø south		file is closed
100330	line P-O		
110620	eol		Foulum
111000	Skallingen	131300	new scanner file
		132500	file is closed
111002	new scanner file "111000.2dd"		
	4 lines over Esbjerg		Roskilde
	120 knots, 1000 ft.		firestation and terminal
111330	clouds over the harbour		120 knots, 500-600 ft.
112615	clouds over the harbour	135159	new scanner file "135200.2dd"
113800	file is closed	140200	apron, file is closed

Bibliography

Arens, C. (2002). Some examples of topographic applications and accuracy of laser scanning. *National Survey and Cadastre—Denmark, Geodetic division, Technical Reports*, 17:66pp.

Bird, E. C. F. (1993). *Submerging coasts*. Wiley and Sons, Chichester.

Christiansen, C., Aagaard, T., Bartholdy, J., Christiansen, M., Nielsen, J., Nielsen, N., Pedersen, J. B. T., and Vinther, N. (2004). Total sediment budget of a transgressive barrier-spit, Skallingen, SW Denmark: A review. *Danish Journal of Geography*, 104(1):107–126.

Forsberg, R., Keller, K., and Jacobsen, S. M. (2001). Laser monitoring of ice elevations and sea/ice thickness in Greenland. *International Archives of Photogrammetry and Remote Sensing*, XXXIV-3/W4:163–168.

Geist, T. and Stötter, J. (2004). Airborne laser-scanning technology for glacial applications—results from the ΩMEGA project. *International Archives of Photogrammetry, Remote Sensing and Spatial Information Sciences*, XXXVI-8/W2.

Haugerud, R. A., Harding, D. J., Johnson, S. Y., Harless, J. L., Weaver, C. S., and Sherrod, B. L. (2003). High-resolution lidar topography of the Puget Lowland, Washington—a bonanza for earth science. *GSA Today*, 13(6):4–10.

Holmgren, J. and Jonsson, T. (2004). Large scale airborne laser scanning of forest resources in Sweden. *International Archives of Photogrammetry, Remote Sensing and Spatial Information Sciences*, XXXVI-8/W2.

Hyyppä, J., Hyyppä, H., Litkey, P., Yu, X., Haggren, H., Rönnholm, P., Pyysalo, U., Pitkänen, J., and Maltamo, M. (2004). Algorithms and methods of airborne laser scanning for forest measurements. *International Archives of Photogrammetry, Remote Sensing and Spatial Information Sciences*, XXXVI-8/W2.

Keller, K., Hvidegaard, S., Forsberg, R., Dalå, N. S., Skourup, H., and Stenseng, L. (2004). Airborne lidar and radar measurements over sea ice and inland ice for CryoSat validation: CRYOVEX 2003—Final report. *National Survey and Cadastre—Denmark, Geodetic division, Technical Reports*, 25:58.

Maas, H.-G. (2002). Methods for measuring height and planimetry discrepancies in airborne laserscanner data. *Photogrammetric Engineering and Remote Sensing*, 68(9):933–940.

Nielsen, N. and Nielsen, J. (2002). Vertical growth of a young backbarrier salt marsh, Skallingen, SW Denmark. *Journal of Coastal Research*, 18:287–299.

Ollson, H. (2004). Summary of the Scandlaser 2003 workshops and recent developments in Sweden. *International Archives of Photogrammetry, Remote Sensing and Spatial Information Sciences*, XXXVI-8/W2.

Sittler, B. (2004). Revealing historical landscapes by using airborne laser scanning—A 3-D model of ridge and furrow in forests near Rastatt (Germany). *International Archives of Photogrammetry, Remote Sensing and Spatial Information Sciences*, XXXVI-8/W2.

Technical Report Series

1. Nynne S. Dalå, René Forsberg, Kristian Keller, Henriette Skourup, Lars Stenseng and Sine M. Hvidegaard.: *Airborne Lidar Measurements of Sea Ice North of Greenland and Ellesmere Island 2004. GreenICE/SITHOS/CryoGreen/A76 Projects. Final Report*, 69 pp., 2005

2. Christian J. Andersen, Nynne S. Dalå, René Forsberg, Sine M. Hvidegaard and Kristian Keller.: *Airborne Laser Scanning Survey of the Wadden Sea Region, Denmark*, 32 pp., 2005